This is a repository copy of *The Response Spectrum Map, Volterra Series Representations and the Duffing Equation.*.

White Rose Research Online URL for this paper:
http://eprints.whiterose.ac.uk/83760/

Monograph:
Billings, S.A. and Boaghe, O.M. (1999) The Response Spectrum Map, Volterra Series Representations and the Duffing Equation. Research Report. ACSE Research Report 754 . Department of Automatic Control and Systems Engineering
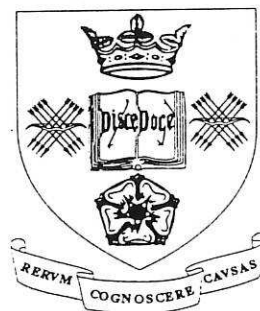
The Response Spectrum Map, Volterra Series Representations and the Duffing Equation

S.A.Billings   O.M.Boaghe

Department of Automatic Control and Systems Engineering
University of Sheffield
Mappin Street, Sheffield S1 3JD
United Kingdom

University of Sheffield

The Response Spectrum Map. Volterra Series Representations and the Duffing Equation

S.A. Billings and O.M. Boaghe

Department of Automatic Control and Systems Engineering, University of Sheffield, PO.Box-600, Mappin Street, S1 3JD. UK

Abstract

The validity of Volterra series representations is assessed in the time and frequency domain for the particular example of the Duffing oscillator. Theoretical results derived in the literature associated with the existence of the Volterra series are reviewed and tested for the Duffing equation. Response Spectrum Maps are introduced for the first time as a frequency domain equivalent to the Bifurcation Diagram. and these are used to qualitatively analyse and detect various dynamical states exhibited by the Duffing oscillator.

1 Introduction

The application of Volterra series and the analysis of power series convergence and truncation for the Duffing equation are the main interest of the current paper. The Volterra representation is useful in practice when a nonlinear system can be adequately described by just a few terms. In other words the Volterra series must converge quickly so that truncating the series does not involve a significant loss of precision.

It is well known that Volterra series exist only for dynamical systems with fading memory. This has been noted by many authors including Volterra [1930], Rugh [1981] and Boyd and Chua [1985]. The requirement of fading memory has been found to be related to the notion of a unique steady state [Boyd and Chua, 1985]. In practice however nonlinear systems can exhibit more complicated dynamics, such as chaotic behaviour. Chaos is common in many nonlinear mechanical and electrical oscillators [Duffing,1918], [Ueda,1980], [Chua,1992]. and has been observed in geomagnetic activity, human physiology, economics and fluid turbulence.

The Duffing equation is chosen as an example in the present study because it arises in the analysis of many physical systems including the pendulum, radio frequency driven Josephson junctions. the bending deflections of an electromagnetically driven steel beam. phase-locked loops. gyroscopes. ferrites. synchronous machines and many other systems. The Duffing oscillator also provides an equation which has been used by many authors as a bench test in the study of nonlinear dynamics.

Closed-form analytical solutions are not available for the Duffing driven nonlinear oscillator. This was discussed for example in Thompson and Stewart [1991] and provided the motivation for extensive investigations, including analogue and numerical simulations together with experimental observations. It has been shown that the Duffing equation exhibits a rich variety of nonlinear bifurcation phenomena and equilibrium points, periodic and chaotic attractors have all been studied.

The existence of a Volterra series for the Duffing equation has been widely discussed in the literature. The main results concluded in Barrett [1963]. Schetzen [1980]. Rugh [1981], Tomlinson et al [1996], Billings and Lang [1997] are reviewed here and the limitations of the Volterra series are outlined. The analysis is performed mainly in the frequency domain, where the frequency domain Volterra series representation has proven to be an excellent descriptor of nonlinear system characteristics. In this context the Response Spectrum Map is introduced for the first time as a frequency domain equivalent to the Bifurcation Diagram. The Response Spectrum Map is shown to be a powerful new tool for the analysis of nonlinear systems behaviour and the application to the Duffing oscillator is described in detail.

The paper is organised as follows: in Section 2 the theoretical background to the Volterra series in both time and frequency domain is briefly reviewed. The Response Spectrum Map is introduced in Section 3 and compared with the Bifurcation Diagram. In Section 4 the analysis of the Duffing oscillator is presented. The Response Spectrum Maps are used to detect mildly nonlinear behaviour where Volterra series can be considered suitable representations.

2   Volterra series in the time and frequency domain

In this section the basic terms and definitions related to Volterra series in both the time and frequency domain are reviewed using the most recent formulations.

The main issues relating to practical applications are summarised, in particular the truncation and approximating properties of Volterra series, and the limits of application are discussed.

Volterra's studies of functionals, representing functions of functions, provided the initial steps in an important field known as functional analysis [Volterra, 1930]. The particular importance of the Volterra series became apparent with Wiener's contribution to nonlinear system analysis. Wiener [1942] applied the Volterra series in an investigation of a nonlinear circuit response by relating the system input $u(t)$ to the output $y(t)$ by a functional series given by

$$y(t) = \sum_{n=1}^{\infty} y_n(t) = \sum_{n=1}^{\infty} \int_{-\infty}^{\infty} \int_{-\infty}^{\infty} \ldots \int_{-\infty}^{\infty} h_n(\tau_1, \tau_2, \ldots, \tau_n) \prod_{i=1}^{n} u(t - \tau_i) d\tau_i \qquad (1)$$

The quantities $h_n(\tau_1, \tau_2, \ldots, \tau_n)$ in equation (1) are known as *kernels of order n*, or *nth-order impulse response functions* of the system.

The initial studies on Volterra series addressed fundamental issues such as existence, convergence and uniqueness. The convergence property formulated in Sandberg [1982] is given as follows. For causal time-invariant nonlinear systems with the Volterra expansion given by (1), where u and y denote the input and output respectively, and each kernel h_n satisfies the integrability condition

$$\int_{0}^{t} \int_{0}^{t} \ldots \int_{0}^{t} |h_n(\tau_1, \tau_2, \ldots, \tau_n)| d\tau_1 d\tau_2 \ldots d\tau_n < \infty \qquad (2)$$

the right side of (1) converges uniformly with respect to t when u satisfies the δ-boundedness condition $|u(t)| \leq \delta$, for $t \geq 0$, where δ is some positive constant that depends on the system considered.

In practical problems only a finite Volterra series can be used, also called a *truncated Volterra series* or *polynomial Volterra series*. Series truncation is made within the limits imposed by the truncation error. A system which is well.described by the first few Volterra kernels and for which the higher order kernels fall off rapidly is generally called a *weakly nonlinear system*. It is straightforward to notice that the input-output Volterra representation of a nonlinear system is useful provided the nonlinearities are only mildly excited so that the number of terms required does not become very large.

Experimental and theoretical methods have been derived in order to find bounds on the time-domain or frequency-domain Volterra kernels for example Chua

and Liao [1991]. Zhang [1996] and Lang [1997]. Recently Sandberg [1999] formulated a Volterra series representation theorem for discrete-time input-output maps that are causal and analytic. which provides a bound on the error in approximating the series with a finite number of terms.

Volterra series have also been considered in the context of causal, time-invariant. nonlinear input-output maps. and not only for systems with an explicit model. For these type of maps approximating Volterra series were sought. This problem has been investigated by many authors, starting with Fréchet [1910], Volterra [1930], Wiener [1958]. Brilliant [1959]. George [1959], and more recently Rugh [1981], Boyd and Chua [1985], Sandberg [1985]. In particular Boyd and Chua [1985] concluded that systems with fading memory may be approximated arbitrarily well by truncated Volterra series. The condition of *fading memory* is a stronger version of continuity [Boyd and Chua, 1985]. Generally speaking a system with fading memory is one for which the dependence on the input decreases rapidly enough with time.

The fading memory requirement however means that the class of systems with multiple equilibria [Boyd and Chua, 1985] cannot be represented by a Volterra model. For these systems a valid unique global Volterra series representation will not exist. Such a system is for example the Duffing oscillator for which three equilibrium points are present in general and in consequence a global unique Volterra series to represent the dynamics around these points does not exist.

However. systems with multiple equilibria may accept local Volterra series representations. Local Volterra series should be valid in a ball of convergence around a certain equilibrium point. In this case a system with multiple equilibria will no longer be described by a unique global Volterra series, but by a few local Volterra series.

From the nonlinear system analysis perspective, the Volterra series kernels are very useful in describing the system input-output behaviour and in finding system properties in a manner which is independent of the inputs. The Volterra kernels have also been studied extensively in the frequency domain. where almost all types of useful mathematical operations in the time-domain are transformed into algebraic operations.

The Fourier transform of the kernels $h_n(\tau_1, \ldots, \tau_n)$ in the Volterra series (1) H_n is called the *nth-order Generalised Frequency Response Function* (GFRF) of the

system [George. 1959]

$$H_n(j\omega_1, \ldots, j\omega_n) = \int\limits_{-\infty}^{\infty} \ldots \int\limits_{-\infty}^{\infty} h_n(\tau_1, \ldots, \tau_n) \epsilon^{-(j\omega_1\tau_1 + \ldots + j\omega_n\tau_n)} d\tau_1 \ldots d\tau_n \qquad (3)$$

The Generalised Frequency Response Function can also be found in the literature with the name *frequency domain Volterra kernel* [Boyd et al. 1984]. or *nonlinear transfer function* [Chua and Ng, 1971(a)].

A frequency domain formula which gives an expression for the output response in terms of the input spectrum and generalised frequency response functions is obtained by replacing the input signal $u(t)$ with the inverse Fourier transform $u(t) = \frac{1}{2\pi} \int\limits_{-\infty}^{\infty} U(j\omega) e^{j\omega t} d\omega$ in the Volterra series (1)

$$
\begin{aligned}
y(t) &= \sum_{n=1}^{\infty} \frac{1}{(2\pi)^n} \int\limits_{-\infty}^{\infty} \ldots \int\limits_{-\infty}^{\infty} H_n(j\omega_1, \ldots, j\omega_n) \prod_{i=1}^{n} U(j\omega_i) e^{j\sum_{i=1}^{n} \omega_i t} d\omega_1 \ldots d\omega_n \\
&= \sum_{n=1}^{\infty} \frac{1}{(2\pi)^n} \int\limits_{-\infty}^{\infty} \ldots \int\limits_{-\infty}^{\infty} Y_n(j\omega_1, \ldots, j\omega_n) e^{j\sum_{i=1}^{n} \omega_i t} d\omega_1 \ldots d\omega_n \qquad (4)
\end{aligned}
$$

where the nth term $Y_n(j\omega_1, \ldots, j\omega_n)$ can be thought of as an n-fold convolution product of U, weighted by $H_n(j\omega_1, \ldots, j\omega_n)$

$$Y_n(j\omega_1, \ldots, j\omega_n) = H_n(j\omega_1, \ldots, j\omega_n) \prod_{i=1}^{n} U(j\omega_i) \qquad (5)$$

The formula (4) describes mathematically the complexity induced by system nonlinearities. While for linear systems the relationship between the input and output spectra is linear, with a frequency range in the output identical with the input components, for nonlinear systems new frequency components are generated, showing nonlinear phenomena described by intra- and inter-kernel interference.

The frequency response function has been studied in relation to the generalised frequency response functions and important properties have been derived in the literature, see for example Chua and Ng [1979 (a) and (b)] where the contributions of the Volterra kernels at a certain intermodulation frequency were determined. The output frequency characteristics have more recently been analysed in Lang and Billings [1996, 1997]. for multi-tone and arbitrary inputs. The frequency domain properties were also related to typical nonlinear phenomena such as nonlinear distortion and interference.

It should be noted that the generalised frequency response function based representation is valid only for systems which admit a Volterra series representation

since the response functions are defined based on the Volterra series. In other words, the predictive property of the representation (4) is only applicable if a Volterra series exists and is convergent for the particular input-output map considered.

3 Bifurcation Diagrams and Response Spectrum Maps

Explicit solutions of the differential equations, such as the Duffing equation, which describe the system in terms of elementary functions or Volterra series are not always possible. In spite of this, geometric interpretation of the differential equations is often undertaken and useful information of a qualitative character can often be obtained.

The geometrical approach of solving differential equations adopted during the last two decades provides useful insight into the realm of nonlinear oscillations. A dynamical system can have a rich variety of solutions: periodic. quasi-periodic or chaotic. It is also common in nonlinear systems to have different coexisting steady-state solutions. or to have several periodic and chaotic motions for the same parameter values but with different initial conditions. Such behaviours can be reflected in the Poincaré Map or Bifurcation Diagram.

In the case of a non-autonomous system. such as the Duffing equation considered in the next section, the Poincaré Map is equivalent to sampling the trajectory of the solution at a rate equal to the forcing frequency [Parker and Chua, 1989]. Fixed points and closed orbits indicate a periodic solution. A fixed point of the Poincaré Map corresponds to a period-one solution and a k-periodic closed orbit corresponds to a kth-order subharmonic.

The Bifurcation Diagram can be seen as a succession of compressed Poincaré Maps. derived for a certain varying parameter. The point r of a Bifurcation Diagram for a non-autonomous system driven by $A cos(\omega t)$ can be defined as [Aguirre and Billings. 1994]

$$ r = \{(y. A) \in \mathbb{R} \times I \quad | \quad y = y(t_i): \ A = A_0: \ t_i = t_0 + K_{ss} \times 2\pi/\omega\} \qquad (6) $$

where I is the interval $I = [A_i: A_f] \subset \mathbb{R}, \ 0 \leq t_0 \leq 2\pi/\omega, \ K_{ss}$ a constant.

However it is often useful to analyse systems in both the time and the frequency domain. As discussed in the previous section, when a nonlinear system

6

can be suitably described by a Volterra series. the Generalised Frequency Response Functions (GFRF) provide useful information about the system dynamics. However the GFRF's cannot be applied to explain complex nonlinear behaviour. such as limit cycles. subharmonics and chaos. In such cases a new analysis. similar to the Bifurcation Diagram. will therefore be introduced to provide insight into the operation of nonlinear systems in the frequency domain. This will be called the Response Spectrum Map.

The Response Spectrum Map (RSM) will be defined as the ensemble of response power spectra corresponding to a nonlinear system response described and generated with a varying parameter. In analogy with the definition of a Bifurcation Diagram stated above for a varying parameter A, the Response Spectrum Map can be defined as

$$S_y : [0; f_N] \times [A_i; A_f] \to \mathbb{R}; \quad S_y(f, A) = S_{y_A}(f) \tag{7}$$

where $S_{y_A}(f)$ is the power spectrum estimated for the system response y_A, when the varying parameter has the value $A \in [A_i; A_f] \subset \mathbb{R}$. The frequency f is varied in the interval $[0; f_N]$, where f_N is the Nyquist frequency.

In practice the Response Spectrum Map is very easy to generate. As in the case of the Bifurcation Diagram. the steady-state system response y_A is required, for a range of values of the parameter A. For each value of A the power spectrum of the system response is computed, using for example the Welch averaged periodogram method. This is repeated for each value of A and a complete map is obtained for the set of values $A \in [A_i; A_f]$. The frequency response map generates a three dimensional plot of the response power spectrum versus frequency and versus A. However a two dimensional representation is obtained if only a plan view or contour plot are considered. The response spectrum is dependent on both the system characteristics and the input properties. As in the case of the Bifurcation Diagram. the Response Spectrum Map is meaningful only if the input is periodic.

It is well known that frequency domain analysis based on the conventional power spectrum has been applied to nonlinear systems showing complex nonlinear behaviour since the formal interpretation of the cascade to chaos. almost two decades ago [Feigenbaum. 1980]. [Cvitanović and Jensen. 1982]. However a response power spectrum mapping of the type introduced in this section has never been used before to the best of our knowledge. The Response Spectrum Map can show the well known cascade to chaos, but more importantly. the map reveals the evolution of the frequency domain features of the system associated with the extra-dimension of the varying parameter and the continuity or discontinuity of these features.

The Response Spectrum Map can be seen as a projection of the information in the Bifurcation Diagram into the frequency domain. Notice that the Bifurcation Diagram and the Response Spectrum Map can be generated at the same time. While the former provides information about the intersection point in the time domain of the flow with a certain plane when a parameter is varied, the latter gives information about the response power spectrum in the frequency domain.

The Response Spectrum Map can be used to identify the various states of a system. States showing complex, strongly nonlinear behaviour, such as subharmonics and chaos are revealed. Mildly nonlinear behaviour, which corresponds to the case where Volterra series can be applied, can also be analysed using the Response Spectrum Map. The main advantage therefore is that the Response Spectrum Map, like the Bifurcation Diagram, is not restricted to the Volterra model class, it can be applied to all nonlinear systems. The insight that this new plot provides will be revealed with examples based on the Duffing model in the next section.

4   Simulation results: The Duffing Equation

The example which will be analysed in detail in this section is the Duffing oscillator. The Duffing model represents a driven damped nonlinear oscillator and was introduced by Duffing in 1918

$$m\ddot{y} + c\dot{y} + k_1 y + k_3 y^3 = u(t) \tag{8}$$

where m, c, k_1 and k_3 are the mass, the damping, and the linear and nonlinear stiffness respectively. This model can for example represent a pendulum where the angle of the pendulum swing is $y(t)$ and the applied torque $u(t)$ is given by $u(t) = A\cos(j\omega_0 t)$.

One of the first studies of the Duffing equation using the Volterra series was by Barrett [1963, 1965]. For the Duffing equation (8) Barrett derived the time-domain Volterra kernels. The first two non-zero terms of the Volterra series were obtained as

$$y(t) = \int_{-\infty}^{+\infty} h_1(t - t_1)u(t_1)dt_1 -$$

$$-k_3 \int_{-\infty}^{+\infty} \int_{-\infty}^{+\infty} \int_{-\infty}^{+\infty} h_3(t - t_1, t - t_2, t - t_3)u(t_1)u(t_2)u(t_3)dt_1 dt_2 dt_3 \tag{9}$$

where

$$h_1(t) = \begin{cases} (\lambda_1 - \lambda_2)^{-1}(e^{\lambda_1 t} - e^{\lambda_2 t}) & \text{for } t > 0 \\ 0 & \text{otherwise} \end{cases} \qquad (10)$$

in which λ_1 and λ_3 are the roots of the characteristic equation $m\lambda^2 + c\lambda + k_1 = 0$ and

$$h_3(t - t_1, t - t_2, t - t_3) = \int_{-\infty}^{+\infty} h_1(t - s)h_1(t - t_1)h_1(t - t_2)h_1(t - t_3)ds \qquad (11)$$

The question of convergence of the Volterra series for the Duffing equation has been analysed by many authors. Barrett [1965] found that in the case where $\frac{k_1}{m} > 0$ and $\frac{c}{m} > 0$ (to ensure stability), if $c^2 \geq 4\frac{k_1}{m}$ the series is convergent (i) for all $u(t)$ when $\frac{k_2}{m} \geq 0$, (ii) when $\frac{k_3}{m} \leq 0$ for all $u(t)$ satisfying

$$max|u(t)| < \frac{2k_1}{3}\sqrt{\frac{k_1}{3|k_3|}} \text{ for } -\infty < t < +\infty \qquad (12)$$

and if $c^2 < 4\frac{k_1}{m}$ the series is convergent for all $u(t)$ satisfying

$$max|u(t)| < \frac{2H}{3}\sqrt{\frac{H}{3|k_3|}} \text{ where } H = k_1 tgh(\frac{\pi}{2}cot\phi) \qquad (13)$$

ϕ being the angle of the complex roots. This result has been confirmed by Christensen [1968].

The Duffing equation has also been analysed in the frequency domain. Schetzen [1980] derived the first Volterra kernel Fourier transforms, which correspond to the time-domain kernels presented above

$$H_1(j\omega_1) = \frac{1}{m(j\omega_1)^2 + c(j\omega_1) + k_1} \qquad (14)$$

$$H_2(j\omega_1, j\omega_2) = 0 \qquad (15)$$

$$H_3(j\omega_1, j\omega_2, j\omega_3) = -\frac{k_3}{3!}H_1(j\omega_1)H_1(j\omega_2)H_1(j\omega_3)H_1\left(j\sum_{i=1}^{3}\omega_i\right) \qquad (16)$$

Because the Duffing equation (8) contains a cubic nonlinear term in $y(\cdot)$, the number of terms in the Volterra series expansion may become infinite. The Volterra series representation used by Barrett [1963] and Schetzen [1981] was truncated after the third order nonlinearity, on the assumption that higher order nonlinearities have an insignificant effect on the system output. The Duffing equation is reduced in this case to a weakly nonlinear system. However there are situations where the input

signal of the oscillator induces significant nonlinear effects making the truncation of the Volterra series and convergence impossible.

By considering only nonlinearities up to the third order the steady-state sinusoidal response is given [Schetzen, 1980] by

$$
\begin{aligned}
y(t) &= A Re\{H_1(j\omega_0)e^{j\omega_0 t}\} + \frac{3A^3}{4} Re\{H_3(j\omega_0, j\omega_0, -j\omega_0)e^{j\omega_0 t}\} \\
&\quad + \frac{A^3}{4} Re\{H_3(j\omega_0, j\omega_0, j\omega_0)e^{3j\omega_0 t}\}
\end{aligned}
\tag{17}
$$

The steady-state response (17) is valid as long as the Volterra series is convergent and the nonlinearities are mild. In other words the output signal $y(t)$ can be predicted from the input signal $u(t)$ and the Fourier transform of the Volterra kernel only for input values included in the Volterra series radius of convergence. In practice the reconstructed signal $y(t)$ is only an estimate of the true $y(t)$, because of truncation effects.

One of the major limitations of the Volterra series representation, as discussed in Section 2, is limited convergence. The Volterra series representation of a physical system may converge for only a limited range of the system input amplitudes. Moreover, the Volterra series can only be applied around stable equilibrium points of the system. In order to assess the implications of these limitations, the convergence domain is analysed next for different sets of parameters in the Duffing equation.

4.1 Location and stability of equilibrium points

The first step in analysing any nonlinear system is often the identification of the equilibrium points [Guckenheimer, Holmes, 1983]. The equilibrium points are the stationary points of the system. Equilibrium points are important because only stable equilibrium points can be observed naturally. Unstable states cannot be realised in any experiment [Guckenheimer, Holmes, 1983]. Moreover Volterra series can only be applied around a stable equilibrium point of the nonlinear system.

For a system of differential equations, the equilibrium states are calculated by setting all the time derivatives to zero in the unforced (autonomous) system. The Duffing equation (8) can then be reformulated as an autonomous system

$$
\ddot{y} + \alpha \dot{y} + \beta y + \gamma y^3 = 0
\tag{18}
$$

by replacing $\alpha = \frac{c}{m}$, $\beta = \frac{k_1}{m}$ and $\gamma = \frac{k_2}{m}$ in (8). The equivalent state space equation

10

for the unforced system is given by

$$\begin{cases} \dot{y} = x \\ \dot{x} = -\beta y - \gamma y^3 - \alpha x \end{cases} \tag{19}$$

If $\frac{\beta}{\gamma} > 0$ there is only one equilibrium point $(x,y)_1 = (0,0)$ and if $\frac{\beta}{\gamma} \leq 0$, there are 3 equilibrium points: $(x,y)_1 = (0,0)$, $(x,y)_2 = (0, \sqrt{-\frac{\beta}{\gamma}})$, $(x,y)_3 = (0, -\sqrt{-\frac{\beta}{\gamma}})$.

The eigenvalues of the Jacobian matrix evaluated at an equilibrium point determine the dynamic behaviour in the neighbourhood of the equilibrium, according to the stable manifold theorem for an equilibrium point. The Jacobian matrix of the system (19) is

$$J = \begin{pmatrix} 0 & 1 \\ -\beta - 3\gamma y^2 & -\alpha \end{pmatrix} \tag{20}$$

By analysing the eigenvalues of the Jacobian J corresponding to each equilibrium point, some relations between local stability properties and parameter values can be established. The conditions for local stability in the Duffing equation (18) case are summarised in Table 1.

Table 1: Local stability conditions for the equilibrium points of the Duffing equation

Equilibrium points	$\alpha^2 - 4\beta \leq 0$		$\alpha^2 - 4\beta > 0$			
	$\alpha > 0, \beta > 0$	$\alpha < 0, \beta > 0$	$\beta > 0$		$\beta < 0$	
			$\alpha < 0$	$\alpha > 0$		
$(0,0)$	stable	unstable	unstable	stable	unstable	

$(0, \pm\sqrt{-\frac{\beta}{\gamma}})$	$\alpha^2 + 8\beta \leq 0$		$\alpha^2 + 8\beta > 0$			
	$\alpha > 0, \beta < 0$	$\alpha < 0, \beta < 0$	$\beta > 0$		$\beta < 0$	
					$\alpha > 0$	$\alpha < 0$
	stable	unstable	unstable		unstable	stable

The stability of the non-autonomous Duffing equation periodic solutions, corresponding in this case to the periodic forcing $u(t) = A\cos(\omega t)$, is mainly discussed in the literature in terms of characteristic (Floquet) multipliers, or from a more geometrical point of view, based on Poincaré Maps.

For the non-autonomous system (8), in the case of a periodic forcing $u(t) = A\cos(\omega t)$, the stability of the periodic response can be further investigated using

Bifurcation Diagrams. The Duffing equation will be analysed for different input amplitude values and considering the parameters m, c, k_1 and k_3 fixed, which produce different dynamics, in the examples below.

4.2   Example 1

The example considered in this section has previously been analysed by Schetzen [1980], as an approximating model for the simple pendulum with linear damping. This example is repeated here for a comparison with the convergence limits derived by Barrett [1965]. The model is

$$\ddot{y} + 6\pi\dot{y} + \omega_0^2(1 + \frac{1}{50})y - \frac{1}{6}\omega_0^2(1 + \frac{1}{50})y^3 = 3 \times 10^3 cos(\omega t) \text{ where } \omega_0 = 30\pi \quad (21)$$

The equilibrium points in this case are $(x, y) = (0, 0)$ which is stable and $(x, y) = (0, \pm\sqrt{6})$ which are unstable, and these are found by using Table 1. In this case a Volterra series may exist around the origin, which is the unique equilibrium point. By applying the formula (13) deduced by Barrett [1965], the Volterra series is convergent for $max|u(t)| \leq 3487.3$. The value chosen for $A = 3 \times 10^3$ is included in the convergence interval and a convergent Volterra series is therefore expected for this example.

By replacing the coefficients of equation (21) in the higher order frequency response function formulas (14-16), it is found that

$$H_1(j\omega) = \frac{1}{(j\omega)^2 + 6\pi(j\omega) + (30\pi)^2\frac{51}{50}} \quad (22)$$

$$H_2(j\omega_1, j\omega_2) = 0 \quad (23)$$

$$H_3(j\omega_1, j\omega_2, j\omega_3) = -\frac{\gamma}{3!}H_1(j\omega_1)H_1(j\omega_2)H_1(j\omega_3)H_1\left(j\sum_{i=1}^{3}\omega_i\right) \quad (24)$$

where $\gamma = -\frac{1}{6}(30\pi)^2\frac{51}{50}$.

After applying the probing method (or harmonic expansion method) [Bedrosian, Rice, 1971], [Peyton-Jones, Billings, 1989] the higher order frequency response functions up to the seventh order can be found

$$H_5(j\omega_1, \ldots, j\omega_5) = -\frac{3!\gamma}{5!}H_1\left(j\sum_{i=1}^{5}\omega_i\right)\sum_{\times} H_3(j\omega_{i_1}, \ldots, j\omega_{i_3})H_1(j\omega_{i_4})H_1(j\omega_{i_5}) \quad (25)$$

$$H_6(j\omega_1, \ldots, j\omega_6) = 0 \quad (26)$$

$$H_7(j\omega_1, \ldots, j\omega_7) = -\frac{\gamma}{7!}H_1\left(j\sum_{i=1}^{7}\omega_i\right)\left(5!\sum_{\times} H_5(j\omega_{i_1}, \ldots, j\omega_{i_5}) + H_1(j\omega_{i_6})H_1(j\omega_{i_7})\right)$$

12

$$+ \quad 3!3!2 \sum_{i=1}^{7} \left(\sum_{**} H_3(j\omega_{i_1}, \ldots, j\omega_{i_3}) H_3(j\omega_{i_4}, \ldots, j\omega_{i_6}) \right) H_1(j\omega_i) \tag{27}$$

where the sum $\sum$ in H_5 is taken over all combinations of 5 coordinates ω_i taken 3 at a time. The first sum $\sum$ in H_7 is taken over all combinations of 7 coordinates taken 5 at a time while the second sum $\sum$ contains all 10 distinct combinations of 6 coordinates taken 3 at a time. in groups of 3.

Schetzen [1980] computes the steady-state response considering nonlinearities up to the fifth order. Here the steady-state response is computed considering nonlinearities up to the seventh order

$$y(t) = y_1(t) + y_3(t) + y_5(t) + y_7(t) \tag{28}$$

where, like in the formula (17). the even order responses make no contribution to the system response. The individual values of the higher order responses are

$$y_1(t) = 2\frac{A}{2} Re\{H_1(j\omega_0)e^{j\omega_0 t}\} \tag{29}$$

$$y_3(t) = 2\left(\frac{A}{2}\right)^3 Re\{H_3(j\omega_0, j\omega_0, j\omega_0)e^{3j\omega_0 t}\} \tag{30}$$

$$+ \quad 6\left(\frac{A}{2}\right)^3 Re\{H_3(j\omega_0, j\omega_0, -\omega_0)e^{j\omega_0 t}\}$$

$$y_5(t) = 2\left(\frac{A}{2}\right)^5 Re\{H_5(j\omega_0, j\omega_0, j\omega_0, j\omega_0, j\omega_0)e^{5j\omega_0 t}\}$$

$$+ \quad 10\left(\frac{A}{2}\right)^5 Re\{H_5(j\omega_0, j\omega_0, j\omega_0, j\omega_0, -\omega_0)e^{3j\omega_0 t}\}$$

$$+ \quad 20\left(\frac{A}{2}\right)^5 Re\{H_5(j\omega_0, j\omega_0, j\omega_0, -\omega_0, -\omega_0)e^{j\omega_0 t}\} \tag{31}$$

$$y_7(t) = 2\left(\frac{A}{2}\right)^7 Re\{H_7(j\omega_0, j\omega_0, j\omega_0, j\omega_0, j\omega_0, j\omega_0. j\omega_0)e^{7j\omega_0 t}\}$$

$$+ \quad 14\left(\frac{A}{2}\right)^7 Re\{H_7(j\omega_0, j\omega_0, j\omega_0, j\omega_0, j\omega_0, j\omega_0. -\omega_0)e^{5j\omega_0 t}\}$$

$$+ \quad 42\left(\frac{A}{2}\right)^7 Re\{H_7(j\omega_0. j\omega_0, j\omega_0, j\omega_0, j\omega_0, -\omega_0. -\omega_0)e^{3j\omega_0 t}\}$$

$$+ \quad 70\left(\frac{A}{2}\right)^7 Re\{H_7(j\omega_0. j\omega_0, j\omega_0, j\omega_0, -\omega_0. -\omega_0, -\omega_0)e^{j\omega_0 t}\} \tag{32}$$

The Duffing equation (21) was simulated using a fourth-order Runge-Kutta algorithm with an integration interval of $1/1800$ and the response $y(t)$ was compared for different levels of approximation given by $\sum_{j=1}^{i(odd)} y_j(t)$, with $y_j(t)$ defined as above in (29-32). The truncation error for different ω values is presented in Table 2, where

Table 2: Different levels of approximation for the stable state response (28) corresponding to the model (21)

ω	ϵ_1 [%]	ϵ_3 [%]	ϵ_5 [%]	ϵ_7 [%]
$\omega = \frac{\omega_0}{5}$	2.41	2.03	2.03	2.03
$\omega = \frac{\omega_0}{3}$	4.82	4.07	4.06	4.06
$\omega = \frac{2\omega_0}{3}$	8.08	7.03	6.99	6.99
$\omega = \omega_0$	53.03	45.08	34.55	30.95
$\omega = \frac{4\omega_0}{3}$	2.74	2.26	2.26	2.26

$e_i(t) = y(t) - \sum_{j=1}^{i(odd)} y_j(t)$, $i \in \{1, 3, 5, 7\}$ expressed as a percentage of the corresponding maximum response.

The Volterra series is convergent, as shown by Table 2. The significance of different higher order terms is found to increase with the amplitude in relation to n, where n is the nonlinearity order. For example, for $\omega = \frac{\omega_0}{5}$, nonlinearities of order higher than 5 do not change the truncation error very much, while for $\omega = \omega_0$, which is the resonant frequency where the response of the system is a maximum, the approximation error is high, even when seventh order nonlinearities are considered.

Schetzen [1980] also remarked that the closer ω is to ω_0 the less rapidly the steady-state of the error $e_i(t)$ decreases with increasing i, and hence higher orders of nonlinearity are required.

Storer and Tomlinson [1993] also observed that at the natural frequency of the linear system, which in this case is $f_0 = 15$ Hz (30π rad/s), distortions of the measured nonlinear transfer functions occur, which increase and become more apparent with an increasing level of the input excitation. The distortions are generated by the increasing significance of the higher order nonlinearities in the steady-state response, and consist of a bending (to the right or left) of the measured (real) transfer function of systems with a hardening or softening stiffness nonlinearity, as the amplitude of the excitation increases.

Figure 1 shows the magnitude of the following frequency response functions: $H_1(j\omega)$ from equation (22), $H_3(j\omega) = H_3(j\omega, j\omega, j\omega)$, which is a projection of the three dimensional function (24) on the axis $\omega_1 = \omega_2 = \omega_3$. $H_5(j\omega) = H_5(j\omega, j\omega, j\omega, j\omega, j\omega)$ from (25) and $H_7(j\omega) = H_7(j\omega, j\omega, j\omega, j\omega, j\omega, j\omega, j\omega)$ in equa-
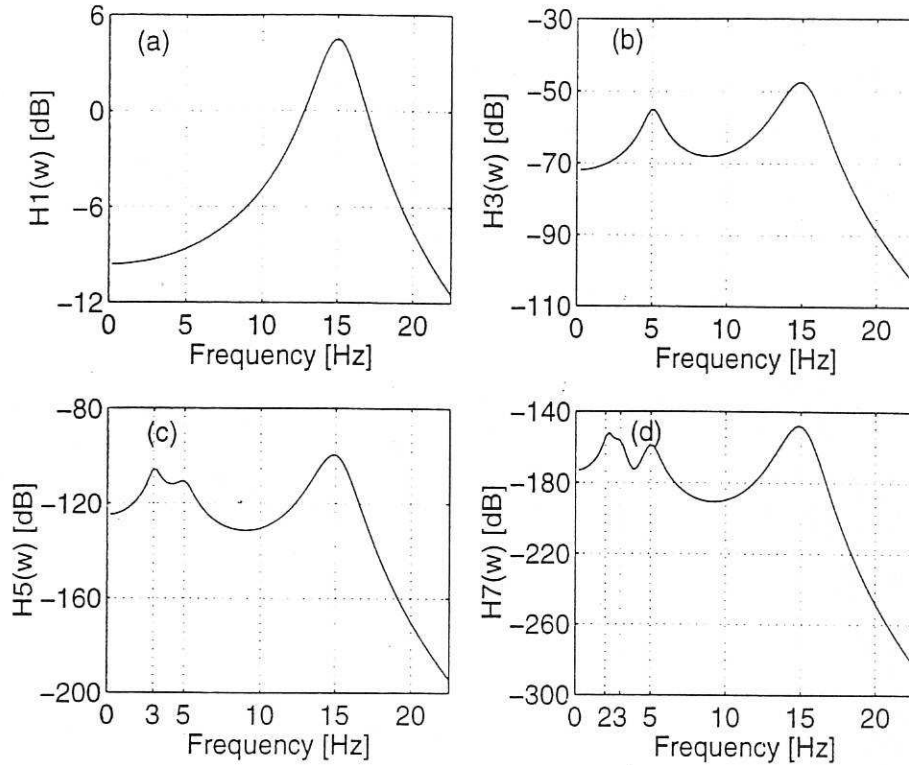
Figure 1: Primary and subharmonic resonances for the higher order frequency response functions of the model (21)

tion (27). The figure shows the local maxima also observed by Schetzen and called subharmonic resonances [Schetzen, 1980, p.152].

For $H_1(j\omega)$ the maximum magnitude value is attained around the primary system resonance $f = f_0 = 15$ Hz. The $H_3(j\omega)$ plot shows two maxima at 15 Hz and 5 Hz, corresponding to the primary and $\frac{1}{3}$ subharmonic resonance. The higher order components $H_5(j\omega)$ and $H_7(j\omega)$ have a supplementary maximum at 3 Hz for the $\frac{1}{5}$ subharmonic resonance and respectively at 2.1 Hz and 3 Hz for the $\frac{1}{5}$ and $\frac{1}{7}$ subharmonic resonances.

4.3 Example 2

The model taken here as an example has been analysed previously by Billings and Lang [1997], in connection with Volterra series truncation

$$m\ddot{y}(t) + c\dot{y}(t) + k_1 y(t) + k_3 y^3(t) = u(t) \tag{33}$$

where $m = 39.2$, $c = 39.2$, $k_1 = 4.9 \times 10^5$, $k_3 = 4.9 \times 10^{10}$, and $u(t) = A\cos(8\pi t)$.

The equilibrium point for the unforced equation is $(x, y) = (0, 0)$ which is stable, therefore the conditions for the existence and uniqueness of a Volterra series are fulfilled. By applying the formula (13) deduced by Barrett [1965], the limit for Volterra series convergence is $A = max|u(t)| \leq 596.40$. This result is in good agreement with the analysis performed in Billings and Lang [1997], where for $A = max(u) = 500$ the truncating order was 3, but for $A = max(u) = 1000$ seventh and even higher order nonlinearities became significant in the system response.

For the present analysis equation (33) was simulated for $u(t) = Acos(8\pi t)$, where $0 \leq A \leq 10000$. A fourth-order Runge-Kutta algorithm with an integration interval of 0.001 was used to simulate the response of the system to the sinusoidal input.

The contributions provided by different orders of nonlinearities are given in Table 3, for different amplitude values. As in the preceding example presented in section 4.2, the truncation error $e_i(t) = y(t) - \sum_{j=1}^{i(odd)} y_j(t)$ is the difference between the simulated output in equation (33) and the estimated stable state from the formula (28), also expressed as a percentage of the corresponding maximum response. It is apparent from Table 3 that the significance of higher order nonlinearities increases with the input amplitude.

Table 3: Different levels of approximation for the stable state response (28) corresponding to the model (33)

Amplitude A	e_1 [%]	e_3 [%]	e_5 [%]	e_7 [%]
$A = 100$	0.6	0.5	0.5	0.5
$A = 500$	14.13	11.39	11.52	11.51
$A = 550$	17.84	14.44	14.65	14.62
$A = 1000$	29.09	21.47	23.79	22.94
$A = 1500$	46.84	25.58	39.95	28.08

The significance of the nonlinear terms can also be analysed in the frequency domain, from the Response Spectrum Map, represented for the varying amplitude $0 \leq A \leq 10000$. These results for both the plan and contour views are shown together with the Bifurcation Diagram in Figure 2.

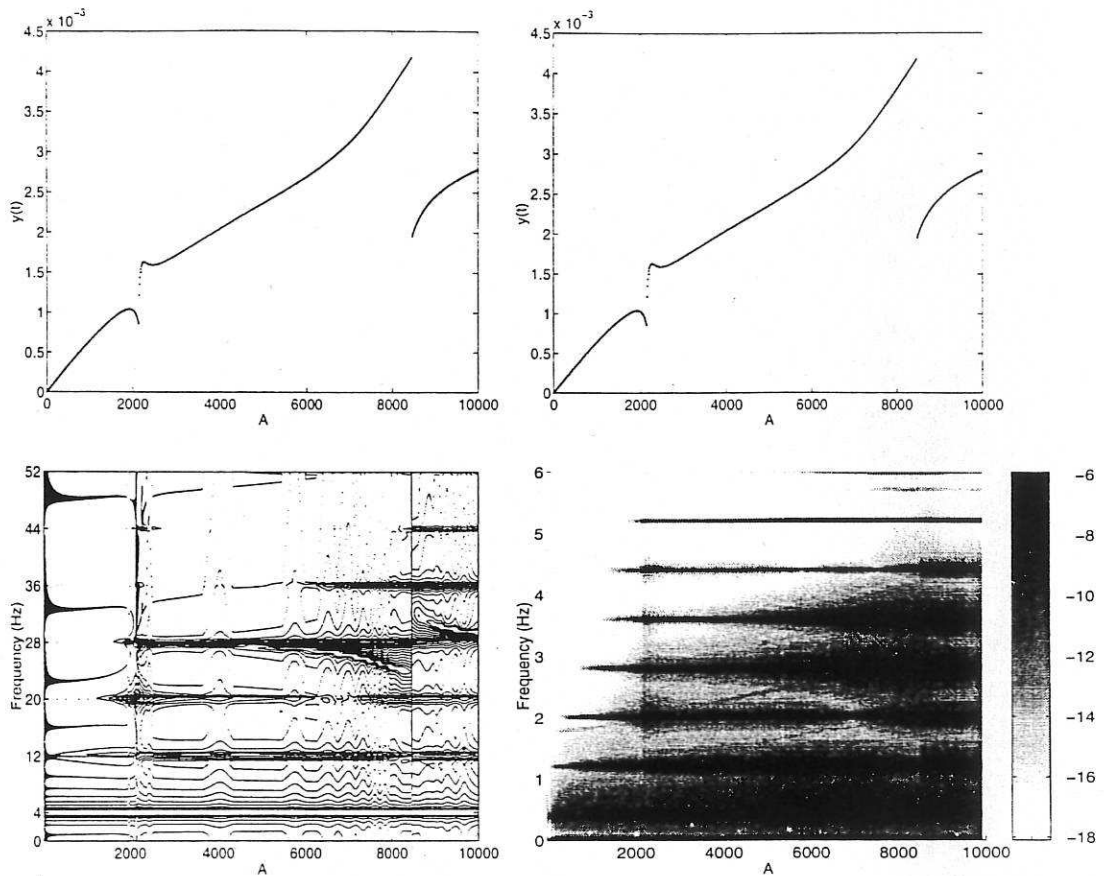The Response Spectrum Map in Figure 2 shows that the output signal consists

Figure 2: Bifurcation Diagram and Response Spectrum Map (plan view and contour plot) for the equation (33)

of spectral terms at the input frequency (0.4 Hz) and at higher (odd) harmonics. Figure 2 confirms in a simple pictorial way the results presented in Billings and Lang [1997]. The Response Spectrum Map shows the significance of the higher order harmonics as the amplitude increases. In particular at $A = 500$ the third order harmonic becomes significant, and similarly. for $A = 1000$ the seventh order harmonic is high in amplitude. as concluded in Billings and Lang [1997].

A comparison of the Response Spectrum Map with the Bifurcation Diagram is also revealing. In Figure 2 the jump resonances occurring at $A = 2150$ and $A = 8460$ are clearly shown in the Response Spectrum Map to generate new high frequency terms. Such information is not evident or predictable from the Bifurcation Diagram. The Response Spectrum Map is therefore complementary to the Bifurcation Diagram and it reveals considerable insight into the complex frequency domain behaviour of a wide class of nonlinear systems.

4.4 Example 3: The Duffing-Ueda equation

The Duffing-Ueda model is a version of the Duffing equation (8), studied extensively by Ueda [1980]

$$\ddot{y} + k\dot{y} + y^3 = u(t) \tag{34}$$

This version of the Duffing equation has no linear stiffness and would arise physically for a beam loaded to precisely its (Euler) buckling load [Thompson, Stewart, 1991]. Once again, for the Duffing-Ueda equation solutions are impossible to derive and digital computations show that after transients have decayed, the system settles down to a condition of steady-state chaos.

By applying the conditions previously found and summarised in Table 1, we can conclude that the Duffing-Ueda equation has only one (0.0) equilibrium point. The corresponding Jacobian matrix is

$$J = \begin{pmatrix} 0 & 1 \\ 0 & -k \end{pmatrix} \tag{35}$$

The eigenvalues of the Jacobian matrix are $\lambda_1 = 0$ and $\lambda_2 = -k$. A zero eigenvalue is considered a special case in ordinary differential textbooks, called degenerate or non-hyperbolic. The dynamics near a degenerate equilibrium point are structurally unstable [Guckenheimer, Holmes, 1983]. The stability of a degenerate or non-hyperbolic point cannot be determined from the eigenvalues (for the autonomous case) or characteristic multipliers (for a period solution) alone [Parker, Chua, 1989]. One possible way of analysing non-hyperbolic equilibrium points is by studying local bifurcations in parameter regions.

For the present analysis the Duffing-Ueda equation (34) was simulated for $k = 0.1$ and $u(t) = A\cos(t)$, where $0 \le A \le 12$. A fourth-order Runge-Kutta algorithm with an integration interval of $\pi/3000$ was used to simulate the response of the system to the sinusoidal input. The input and output signals were further sampled at periods of $T_s = \pi/60$ sec.

The Bifurcation Diagram of the simulated model is presented in Figure 3. The parameter which was varied was the amplitude of the sinusoidal input which was varied in the range $0 \le A \le 12$. This diagram gives a precise indication of how the system bifurcates as the amplitude is varied.

A very detailed and comprehensive diagram of the Duffing-Ueda dynamic regimes was provided by Ueda [1980], where various attractors of the final motions are displayed, depending on the system parameters $0 \le k \le 0.8$ and $0 \le A \le 25$, as

18

well as on the initial conditions. One region in the $k - A$ plane may have multiple attractors. each attractor having its own ensemble of starting conditions. Moreover periodic and chaotic attractors may coexist in the same $k - A$ region.

The Response Spectrum Map, for a varying amplitude A of the input signal $u(t) = A\cos(t)$ is also given in Figure 3. The map is represented as a plan view of the response power spectra and this shows only the relevant features. The frequency of the sinusoidal input $f = 1/(2\pi) = 0.159$ Hz is present for all amplitude A values. The map clearly reflects various regimes such as subharmonic generation and chaotic states and confirms the results previously obtained by Ueda [1980].
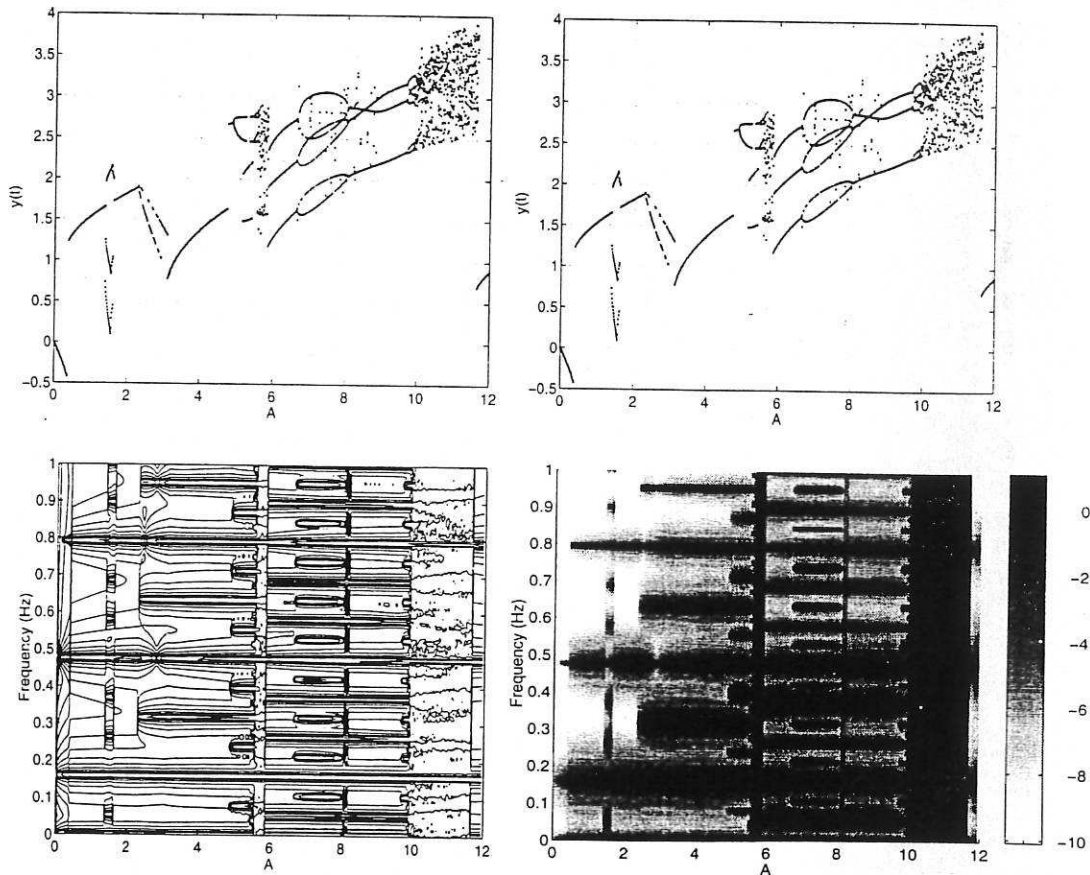
Figure 3: Bifurcation Diagram and Response Spectrum Map (plan view and contour plot) for the Duffing-Ueda equation (34)

The map shows a subharmonic of order $\frac{1}{3}$ at 0.053 Hz and a subharmonic of order $\frac{5}{3}$ at 0.265 Hz in the amplitude range $1.39 \leq A \leq 1.61$. where a $\frac{1}{3}$ and a $\frac{5}{3}$ order subharmonic should be present according to Ueda. A superharmonic of order 2 appears at 0.315 Hz for $3.12 \leq A \leq 4.86$, and this is the 2nd-order superharmonic

found by Ueda for the same amplitude interval. In the interval $5.82 \leq A \leq 9.67$ there is a subharmonic of order $\frac{1}{3}$ at 0.053 Hz and one of order $\frac{2}{3}$ at 0.106 Hz. in the interval $6.67 \leq A \leq 8.03$. Two windows of chaos appear in the intervals $5.55 \leq A \leq 5.82$ and $9.94 \leq A \leq 11.64$ and are easy to recognise by the almost continuous spectrum. Both windows of chaos are preceded by cascades to chaos of order $\frac{1}{2^n}$ and $\frac{1}{3*2^n}$ respectively.

4.5   Example 4: The Duffing-Holmes equation

Another very well known version of the Duffing equation is the Duffing-Holmes equation. Introduced by Holmes [1979], the equation has been used to model mechanical oscillations arising in two-well potential problems [Moon, 1987]

$$\ddot{y} + \alpha\dot{y} + \beta y + y^3 = A cos(\omega t), \text{ where } \beta = -1 \tag{36}$$

The location and stability of the equilibrium points is first considered, for no external forcing. $A = 0$. By analysing the results summarised in Table 1 it is easy to conclude that for $\beta = -1$ and $\alpha = 1.5$ there are two stable equilibrium points at $(x, y) = (0, \pm\sqrt{-\beta}) = (0, \pm 1)$, and one unstable equilibrium at $(x, y) = (0, 0)$.

The non-autonomous case has been analysed in the literature. see for example Guckenheimer and Holmes [1983] or Aguirre and Billings [1995]. The Bifurcation Diagram was further analysed for the particular case $\alpha = 1.5$. $\beta = -1$ and $\omega = 1$ rad/sec

$$\ddot{y} + 1.5\dot{y} - y + y^3 = A cos(t) \tag{37}$$

This equation was simulated using a fourth-order Runge-Kutta algorithm with an integration interval of $\pi/15$, for an amplitude A varying in the range $1 \leq A \leq 1.6$. The Bifurcation Diagram is shown in Figure 4. The Bifurcation Diagram shows a series of flip bifurcations. also referred to as period doubling or subharmonic bifurcations [Guckenheimer, Holmes, 1983]. The first flip bifurcation appears at $A = 1.1$, with a subcritical counter-part at $A = 1.51$. A second flip bifurcation occurs at $A = 1.25$. with the subcritical bifurcation at $A = 1.42$. As A continues to increase. a further bifurcation occurs at $A = 1.29$ with the corresponding subcritical point at $A = 1.38$. These bifurcations accumulate at a point at which transition from periodic to incomplete cascade to chaos occurs. in the window $1.32 \leq A \leq 1.36$.

The corresponding Response Spectrum Map is also given in Figure 4. For each flip bifurcation a new subharmonic is produced. In the interval $1.1 \leq A \leq 1.51$

20

a $\frac{1}{2}$ subharmonic appears at 0.078 Hz. generated by the first flip bifurcation. A $\frac{1}{4}$ subharmonic is further generated at 0.039 Hz in the interval $1.25 \leq A \leq 1.42$. and $\frac{1}{8}$ subharmonics appear at 0.019 Hz for $1.29 \leq A \leq 1.38$. The incomplete cascade to chaos is represented by an almost continuous spectrum in the range $1.32 \leq A \leq 1.36$.

The conventional power spectra of the output are represented in Figure 5 for
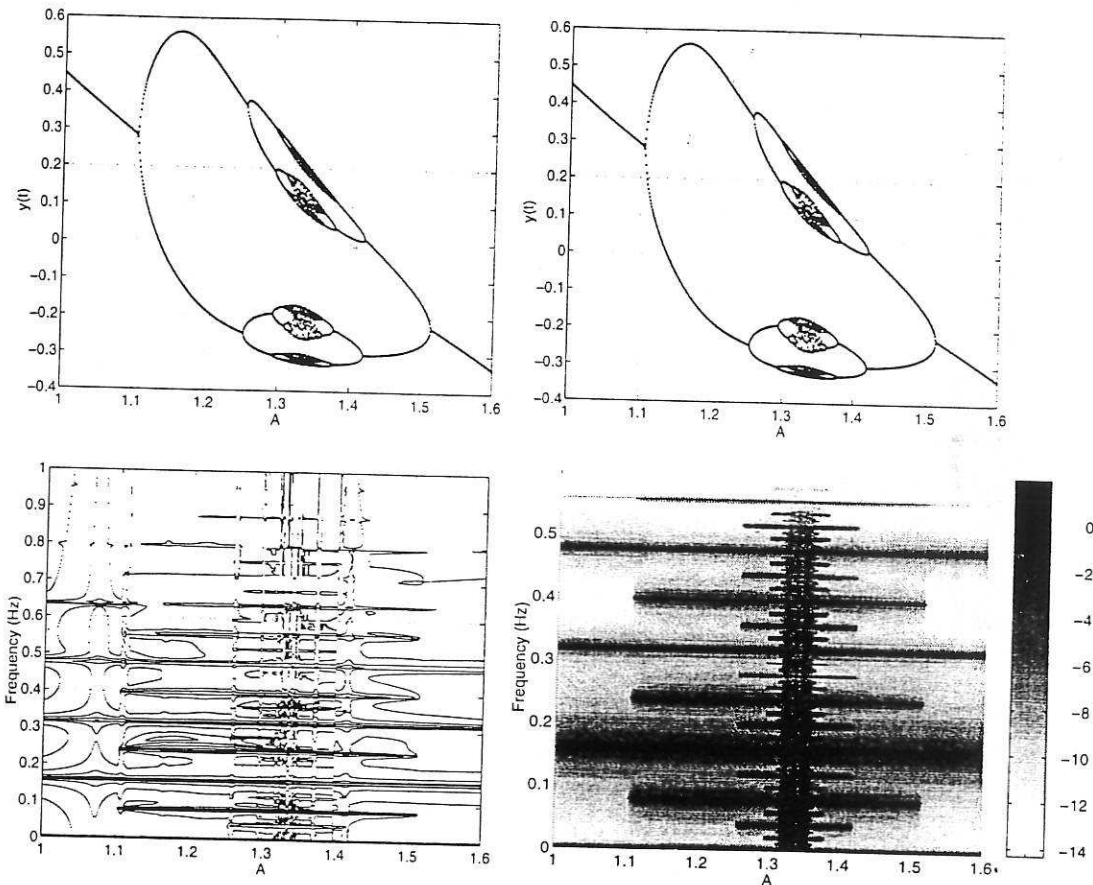

Figure 4: Bifurcation Diagram and Response Spectrum Map (plan view and contour plot) for the Duffing-Holmes equation (37)

the amplitude values corresponding to the flip (subharmonic) bifurcations. The subharmonic halving can be followed from Figure 5 (a) to (d). Such cascades of period doubling bifurcations have been studied extensively and have many interesting universal properties. Feigenbaum analysed the response power spectrum of a period-doubling sequence for the Duffing equation in Feigenbaum [1980] where it was concluded that for every subharmonic halving there is a drop of 8.2 dB in the subharmonic power spectrum.
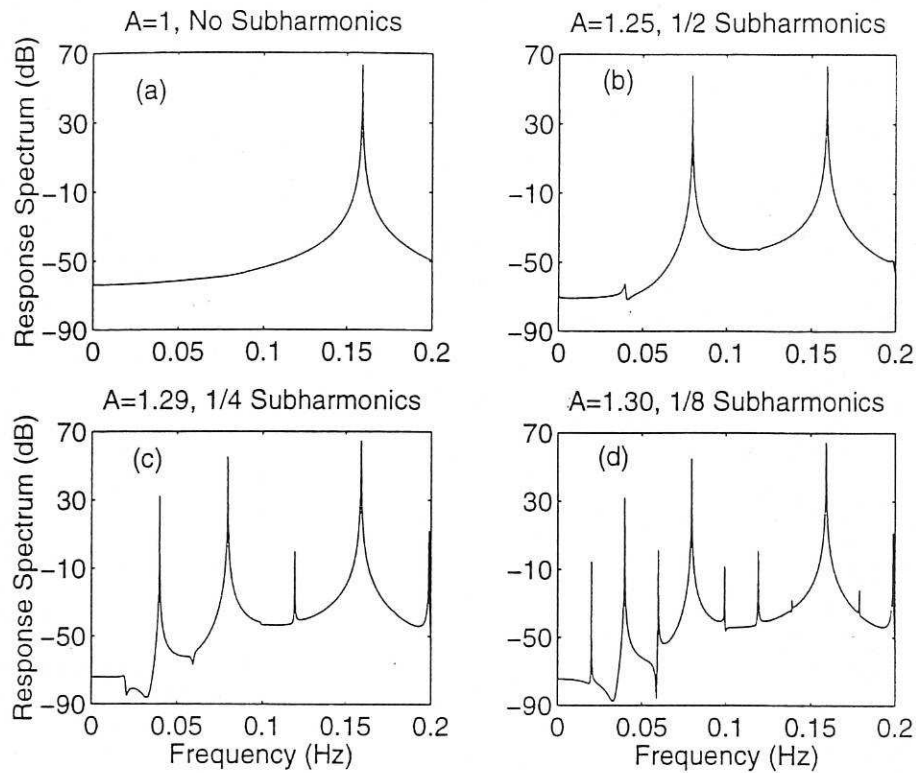
Figure 5: Response power spectra for different subharmonic bifurcations of the Duffing-Holmes equation (37)

5 Conclusions

The objective of this paper was to introduce the Response Spectrum Map and to investigate the modelling limitations of the Volterra series using the Duffing oscillator as an example. Mildly nonlinear systems can be studied by analysing just the first few terms in the Volterra series. In these cases inspection of the kernel plots or the equivalent Generalised Frequency Response Functions provides a complete characterisation of the system properties.

However the Volterra series has limitations and it can only be used to model severely nonlinear systems around the equilibrium points within a relatively small area of convergence. Four cases of the Duffing oscillator were used to illustrate these effects. Outside the Volterra convergence area the Duffing equation dynamics can be much more complex. Phenomena associated with strong nonlinearities are generated including limit cycles. subharmonics and chaos.

The Response Spectrum Map was introduced for the first time as a simple

visual aid to interpreting these effects in the frequency domain. The advantage of the Response Spectrum Map is that is easy to compute and it provides a pictorial display of the system characteristics which is complementary to the Bifurcation Diagram. The Duffing model examples clearly show that a combined analysis and interpretation of both the Bifurcation Diagram and the Response Spectrum Map provides a very clear insight into the operation of even very complex nonlinear systems.

6   Acknowledgements

References

[1] Aguirre. L.A.. Billings. S.A.. 1994. "Validating identified nonlinear models with chaotic behaviour", International Journal of Bifurcation and Chaos. Vol.4. No.1. pp.109-125.

[2] Aguirre, L.A.. Billings. S.A., 1995, "Retrieving dynamical invariants from chaotic data using NARMAX models", International Journal of Bifurcation and Chaos, Vol.5, No.2. pp.449-474.

[3] Barrett, J.F., 1963, "The use of functionals in the analysis of nonlinear physical systems", Journal of Electronic Control, Vol.15, pp.567-615.

[4] Barrett, J.F., 1965, "The use of Volterra series to find the region of stability of a nonlinear differential equation", International Journal of Control, Vol.1, pp.209-216.

[5] Bedrosian, E., Rice, S.O, 1971, "The output properties of Volterra systems (nonlinear systems with memory) driven by harmonic and Gaussian inputs", Proceedings of the IEEE, Vol.59. No.12, pp.1688-1707.

[6] Billings. S.A.. Lang, Z.Q., 1997. "Truncation of nonlinear systems in the frequency domain". International Journal of Control. Vol.68. No.5. pp.1019-1042.

[7] Boyd. S., Chua. L.O., Desoer, C.A., 1984, "Analytical Foundations of Volterra Series", IMA Journal of Mathematical Control & Information. Vol.1, pp.243-282.

[8] Boyd, S., Chua. L.O., 1985, "Fading Memory and the Problem of Approximating Nonlinear Operators with Volterra Series", IEEE Transactions on Circuits and Systems. CAS-32, No.11, pp.1150-1161.

[9] Brilliant, M.B.. 1959, "Theory of the analysis of nonlinear systems", MIT Research Lab. of Electronics. Technical Report No.345.

[10] Christensen, G.S.. 1968. "On the convergence of Volterra series". IEEE Transactions on Automatic Control, Vol.13, pp.736-737.

[11] Chua. L.O., 1992, "The genesis of Chua's circuit". Archiv für Electronik und Übertrangungstechnik. Vol.46. No.4. pp.250-257.

[12] Chua. L.O.. Liao. Y., 1991. "Measuring Volterra kernels (III)". International Journal of Circuit Theory and Applications, Vol.19, pp.189-209.

[13] Chua. L.O.. Ng. C.Y.. 1979(a), "Frequency domain analysis of nonlinear systems: General theory". Electronic Circuits and Systems. Vol.3. No.4, pp.165-185.

[14] Chua, L.O.. Ng, C.Y.. 1979(b), "Frequency domain analysis of nonlinear systems: Formulation of transfer functions", Electronic Circuits and Systems, Vol.3. No.6. pp.257-269.

[15] Cvitanović, P., Jensen, H., 1982, "Universality in chaos". published in "Universality in chaos", Ed. Predrag Cvitanovic, pp.3-34, 1989.

[16] Duffing, G., 1918, "Erzwungene Schwingungen bei Weranderlicher Eigenfrequenz", Vieweg: Braunschweig.

[17] Feigenbaum, M.J., 1980, "Universal behaviour in nonlinear systems", Los Alamos Science, Vol.1. pp.4-27, in "Universality in chaos", Ed. Predrag Cvitanovic, pp.49-84, 1989.

[18] Fréchet, M., 1910, "Sur les functionelles continues". Ann. l'École Normale Sup., Vol.27.

[19] George, D.A.. 1959, "Continuous nonlinear systems". MIT Research Lab. of Electronics. Technical Report No.355.

[20] Guckenheimer. J.. Holmes, P., 1983. "Nonlinear oscillations. dynamical systems and bifurcation of vector fields", Springer-Verlag, New-York.

[21] Holmes, P.J., 1979, "A nonlinear oscillator with a strange attractor", Communications in Mathematical Physics, Vol.50, pp.69-77.

[22] Lang, Z.Q., Billings, S.A, 1996, "Output frequency characteristics of nonlinear systems". International Journal of Control, Vol.64. No.6. pp.1049-1067.

[23] Lang, Z.Q.. Billings. S.A. 1997, "Output frequency of nonlinear systems". International Journal of Control, Vol.67. No.5. pp.713-730.

[24] Moon. F.C.. 1987. "Chaotic vibrations - An introduction for applied scientists and engineers". John Wiley. New-York.

[25] Parker. T.S.. Chua. L.O.. 1989, "Practical numerical algorithms for chaotic systems". Springer-Verlag. New-York.

[26] Peyton-Jones, J.C., Billings, S.A., 1989, "Recursive algorithm for computing the frequency response of a class of non-linear difference equation models", International Journal of Control, No. 50, pp.1927-1942.

[27] Rugh, W.J., 1981, "Nonlinear system theory - The Volterra / Wiener approach", The John Hopkins University Press.

[28] Sandberg, I.W., 1982, "Volterra expansions for time-varying nonlinear systems", Bell Systems Technical Journal, Vol.61, No.2, pp.201-225.

[29] Sandberg, I.W., 1985, "Nonlinear input-output maps and approximate representations", AT&T Technical Journal, Vol.64, No.8, pp.1967-1983.

[30] Sandberg, I.W., 1999, "Bounds for discrete-time Volterra series representations", IEEE Transactions on Circuits and Systems - I Fundamental Theory and Applications, Vol.46, No.1, pp.135-139.

[31] Schetzen, M., 1980, "The Volterra and Wiener theories of nonlinear systems", John Wiley and Sons, New York.

[32] Soliman, S.M., Thompson, J.M.T., 1992, "Indeterminate trans-critical bifurcations in parametrically excited systems", Proceeding of the Royal Society of London, A, Vol.439, No.1907, pp.601-610.

[33] Storer, D.M., Tomlinson, G.R., 1993, "Recent developments in the measurement and interpretation of higher order transfer functions from nonlinear structures", Mechanical Systems and Signal Processing, Vol.7, No.2, pp.173-189.

[34] Thompson, J.M.T., Stewart, H.B., 1991, "Nonlinear dynamics and chaos", John Wiley and Sons, New York.

[35] Tomlinson, G.R., Manson, G., Lee, G.M., 1996, "A simple criterion for establishing an upper limit to the harmonic excitation level of the Duffing oscillator using Volterra series", Journal of Sound and Vibration, Vol.190, No.5, pp.751-762.

[36] Ueda, Y., 1980, "Steady motions exhibited by Duffing's equation: a picture book of regular and chaotic motions", in New Approaches to Nonlinear Problems in Dynamics, Ed. P.J.Holmes, SIAM: Philadelphia, pp.311-322.

[37] Volterra, V., 1930, "Theory of functionals and of integral and integro-differential equations", Blackie and Sons Ltd, London.

[38] Wiener, N., 1942, "Response of a non-linear device to noise", MIT Radiation Laboratory Report, V-16S.

[39] Wiener, N., 1958, "Nonlinear problems in random theory", John Wiley and Sons. MIT Press, New York.

[40] Zhang, H., Billings, S.A., 1996, "Gain Bounds of higher-order nonlinear transfer functions", International Journal of Control, Vol.64, No.4, pp.767-773.